Received: 26 July 2018 | Revised: 22 October 2018 | Accepted: 4 November 2018
DOI: 10.1002/ardp.201800221

FULL PAPER

DPhG ARCH PHARM
Archiv der Pharmazie

Efficient synthesis of *meso*-substituted porphyrins and molecular docking as potential new antioxidant and cytotoxicity agents

Sraa Abu-Melha

Faculty of Science of Girls, Department of Chemistry, King Khaled University, Abha, Saudi Arabia

Correspondence
Sraa Abu-Melha, Faculty of Science of Girls, Department of Chemistry, King Khaled University, Abha 35516, Saudi Arabia.
Email: sraa201313@yahoo.com

Abstract

An improved methodology is reported for the synthesis of new series of mesotetrakis-[aryl]-21*H*,23*H*-porphyrin derivatives **2a–h** and was considered as a model to study their antioxidant and cytotoxic activities. The structures of the novel compounds were determined in ^{1}H and ^{13}C NMR, UV-Vis, and elemental analyses. Among the derivatives, compounds **2c**, **2d**, and **2h** showed strongest radical-scavenging activity. Moreover, according to our results, compounds **2c**, **2d**, **2g**, and **2h** have very strong activity against the HepG2 hepatoma cell line, with IC_{50} values from 9 to 25 μg/mL. Molecular docking was performed to investigate the binding between the most active porphyrin derivatives **2c**, **2d**, **2g**, **2h** and the two molecular targets Bcl-2 and caspase-3. Compounds **2c** and **2d** seem to have better affinities to both proteins than **2g** and **2h**.

KEYWORDS
aldehydes, antioxidant, cytotoxicity, molecular docking, porphyrins, pyrrole

1 | INTRODUCTION

The porphyrins have been recognized as one of the most important prosthetic groups in biological systems. The diverse chemistry performed by natural porphyrins has inspired works in various fields of chemistry.[1] In the past decades, much interest has been focused on the synthesis of well-defined porphyrins for potential application as photosensitizer in photodynamic therapy (PDT) of cancer.[2] Though there are many aspects to attain to this purpose, one important issue to porphyrin derivatives is their availability. Up to now, the most porphyrins investigated are obtained from naturally occurring porphyrins like hematoporphyrin and protoporphyrin, involving complicated modification reaction and tedious separation. Porphyrin-type compounds have been actively investigated as sensitizing drugs for application in cancer diagnosis and treatment using photodynamic therapy and also using boron neutron capture therapy (BNCT).[3] Porphyrins have been reported to possess a variety of biological and pharmacological activities. The desirable cancer preventive or putative therapeutic properties of porphyrins have also been considered to be associated with their antioxidant properties, since free radical-mediated peroxidation of membrane lipids and oxidative damage of DNA were believed to be associated with a variety of chronic health problems, such as cancer, atherosclerosis, neurodegenerative diseases, and aging.[4] Therefore, the past few years have witnessed intense research devoted to the antioxidant activity of porphyrin. For instance, studies pertaining to the kinetics and mechanisms of natural antioxidants[5] have demonstrated that simple structural modifications of resveratrol, which is an antioxidative component in red wine, could significantly enhance its antioxidative activity[6] and cytotoxicity against cancer cells.[7] This motivated us to use porphyrin as a lead compound to design more active potential antioxidants and chemopreventive agents against cancer.

Porphyrins substituted at the *meso*-position have been synthesized and used as molecular materials.[8,9] The synthesized porphyrins

showed interesting physicochemical properties, electrochemical characters, medical treatment,[10] photosensitizers,[2] photocatalysts[11] and wide range of different technology. The general methods for the synthesis of porphyrins involved condensation of dipyrromethanes with different aldehydes in acid medium. Most of the reported methods led to the formation of porphyrins in low yields due to the side reactions and the formation of polymeric products. It has been published that porphyrins have different biological and pharmacological activities. This prompted us to synthesize new porphyrin derivatives to be used as antioxidant and anticancer agents.

2 | RESULTS AND DISCUSSION

2.1 | Chemistry

Many methods deal with the synthesis of porphyrin derivatives.[8] All the reported methods have two long standing problems associated with low yield reactions (6:20%) and purification.[12] In our lab, we synthesized new porphyrin derivatives in very good yield 70:85% with successful purification on silica gel using eluent (1.5:1 chloroform/hexane). We successfully used the capping process which prevents the formation of polymeric pyrrole. We used DMF as solvent and capping agent.[13]

It involves the acid-catalyzed addition of the pyrrole to the substituted benzaldehyde carbonyl group followed by acid-catalyzed dehydration. Repeating this process adds the next benzaldehyde moiety. Ring closure results in the formation of the reduced form of porphyrin (porphyrinogen) followed by oxidation to furnish the porphyrin building blocks. In the presence of DMF, a reversible cap forms which protects this intermediate species, while allowing the reaction with pyrrole.

Aldehyde derivatives **1a–h** were condensed with pyrrole in presence of *p*-toluenesulfonic acid in DMF as solvent and capping agent afforded the porphyrin derivatives **2a–h**. The rate and yield of reaction depend on the concentration of *p*-toluenesulfonic acid, solvent, temperature, and the presence of atmospheric oxygen and initial concentration of reactants (Scheme 1). Schemes 2 and 3 show the reaction capping mechanism.

The relation between the observed absorption maximum shifts and the polar characteristics of substituents is shown in Table 1. From Table 1, it was noticed that there is no any increase or decrease in λ_{max} in the visible region and there is no any marked change for log ε due to the presence of electron donating or electron withdrawing groups.

2.2 | Pharmacology

2.2.1 | Antioxidant activities

The newly synthesized compounds **2a–h** were evaluated for their antioxidant properties. We used 2,2-diphenyl-1-picrylhydrazyl (DPPH) assay. The purple-colored radical DPPH$^{\bullet}$ was reduced to yellow-colored DPPH-H form (Table 2) by all tested compounds. We used 3,5-di-*tert*-butyl-4-hydroxytoluene (BHT) and 3-*tert*-butyl-4-hydroxyanisole (BHA) as positive controls. The results showed that compounds **2c**, **2d**, and **2h** have strongest antioxidant activity. This high antioxidant activity of compounds **2c** and **2d** can be attributed to the presence of nitrogen and sulfur atoms in their structures. This result agrees with the previously reported work showing that the sulfur atom in porphyrin derivatives acts as good radical scavenger.[14] The deoxyribose assay was used to measure the hydroxyl radical scavenging activity of the synthesized compounds (Table 2). Protective effect of the new compounds was followed as they can remove hydroxyl radicals from the tested solution and inhibit the degradation. It was found that all tested compounds, especially **2c**, **2d**, and **2h** have high prevention of degradation. IC_{50} values of compounds **2c**, **2d**, and **2h** showed that they are very strong scavengers of OH radicals (generated in Fenton's reaction). The prevention of lipid peroxidation (LP) was characterized by determining the formation of MDA, using liposomes as an oxidizable substance.[15] Compounds **2c** and **2d** showed the highest inhibition of some of Fe^{2+}/ascorbate-induced LP in liposomes. From Table 2, it was noticed that compounds **2c** and **2d** are very good inhibitors of LP and the most active compounds in this assay as antioxidant agents comparable to the positive controls. These results showed great agreement with the previous reported work that sulfur compounds are good antioxidants at low concentration.[14]

2.2.2 | Cytotoxic activity of new porphyrin derivatives against human cell lines

The porphyrin mode(s) of action, their cytotoxicity are due to caspase 3/7 activation and subsequent induction of apoptosis. Additionally, different phenotypical changes were observed and these included endoplasmic reticulum, actin cytoskeleton, and cellular morphology alterations as well as cell cycle arrest and various biochemical changes (e.g., ROS and GSH levels).[16–19]

The cytotoxicity of the newly synthesized compounds are tested against HepG2, MCF-7, Vero and normal cells (WI-38) and their effect on the expression levels of caspase-3 and Bcl-2 molecular biomarkers is evaluated.

The metabolic activity of the cells was measured after 48 h of incubation with different concentrations of the investigated compounds by means of MTT assay. The IC_{50} (μM) was determined from the dose–response curves as mean of two parallel experiments; 5-fluorouracil (5-Fu) was used as positive control; growth inhibition 100 μM (inactive).

2.2.3 | Structure–activity relationship

From Table 3, it was noticed that compounds **2c** and **2d** displayed the highest cytotoxic activity against HepG2 cell line. Also, compounds **2g**, **2h**, and **2b** showed cytotoxic activity against the same cell line. The rest of other compounds exhibited low activity against HepG2. From these results, we can conclude that sulfonyl group enhances the cytotoxic activity against all cell lines. Moreover, it was found that compounds **2c** and **2d** displayed the strongest cytotoxic activity against WI-38 cell

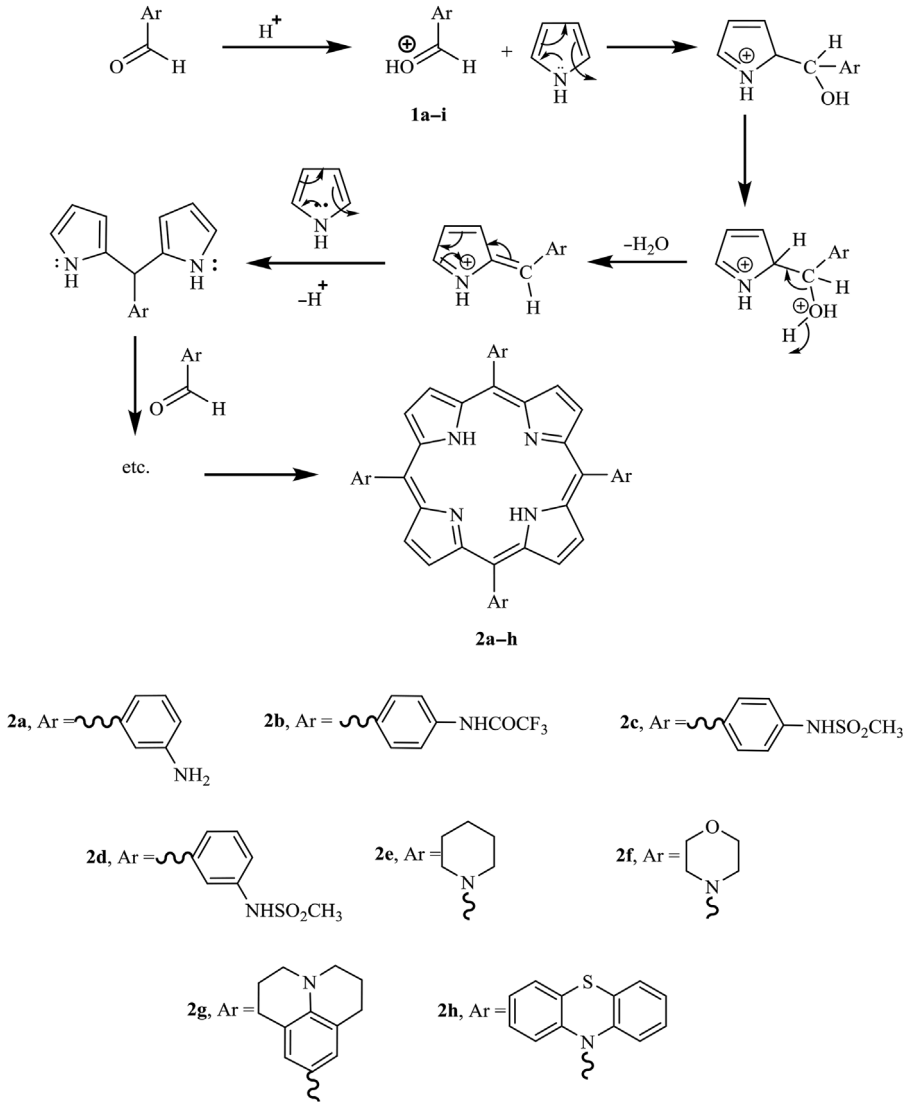

SCHEME 1 Synthesis of porphyrin derivatives **2a–h**

line in which these results were attributed to the effect of sulfonyl group present in their structure. Compound **2b** displayed mild cytotoxicity due to the presence of fluorine atom in its structure, which acts as electron withdrawing group, the rest of other compounds exhibited weak activity. Compounds **2h**, **2c**, and **2d** displayed good activity against Vero cell line, while the other compounds exhibited weak cytotoxicity against the same cell line. In addition, compounds **2c** and **2d** showed the highest activity against MCF-7 cell line owing to the sulfonyl group and rich in nitrogen atom.

Of course, such initial studies are not directly transferable and therefore require more investigations using a wider arsenal of normal and tumor cells, and eventually organismic experiments.

2.2.4 | Evaluation of caspase-3 and Bcl-2 molecular biomarkers in HepG2 cells

In order to further study the possibly addressed signaling pathways and obtain hints on the mode(s) of action of the most promising compounds **2c**, **2d**, **2g**, and **2h** at the molecular level, the expression levels of selected tumor proliferation, anti-apoptotic and apoptotic protein markers were assessed in HepG2 cells. In view of the former, pro-apoptotic caspase-3 and anti-apoptotic Bcl-2 proteins were selected to monitor apoptosis induction.

As shown in Figure 1, compounds **2c**, **2d**, **2g**, and **2h** were able to upregulate the expression of caspase-3 and down regulate the expression of Bcl-2 compared with untreated cells. It is worthwhile to mention that a distinct correlation was observed between the chemical structures of test compounds and their corresponding expression modulation activity showing that it is not a general porphyrin cytotoxic effect. Not surprisingly, and in agreement with SARs.

Interestingly, **2d** exhibited a superior activity within its series analogues and this worth further study. These results were in line with our previous studies, in which porphyrin-based aromatic amine derivatives induced a chain of biochemical alterations among which is the cell caspases activation and apoptosis induction.[12,20,21] These

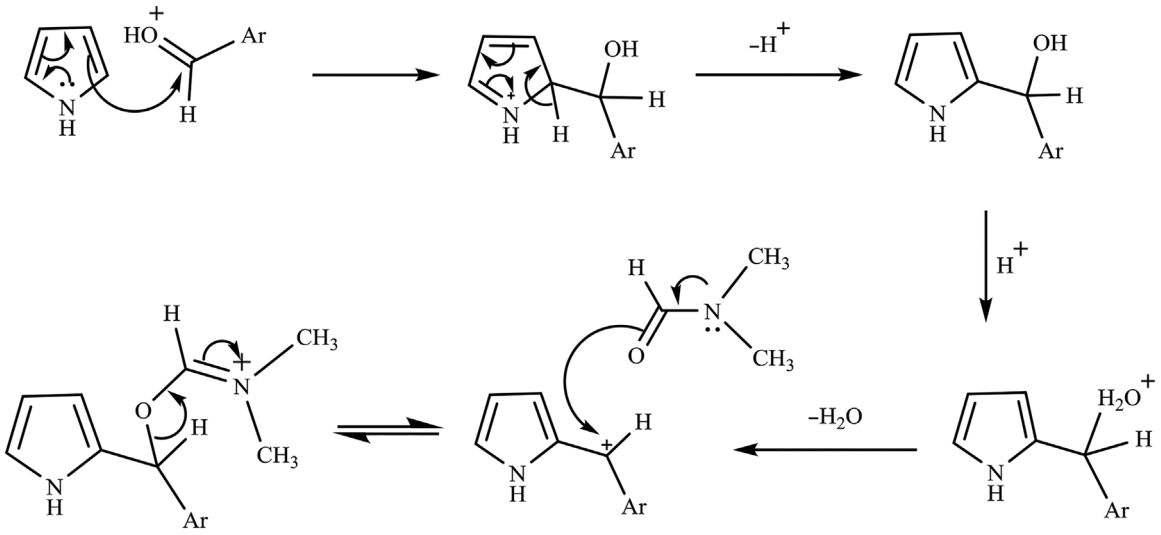

SCHEME 2 Proposed nucleophilic attack by pyrrole on protonated aldehyde following nucleophilic attack by the DMF nitrogen on the carboncation to form a reactive species with DMF as a good leaving group of DMF as a capping agent during porphyrin formation

alterations seem to take place primarily in specific cells (e.g., HepG2) with a disturbed intracellular redox balance.

While it is premature to explain why compound **2d** was among the most active agents in these assays, one may speculate that this compound may hit more than one specific cellular target(s) and cause widespread modification of proteins and enzymes for the benefit of activation. Furthermore, it is likely that **2d** might also be taken up by cells and modified *in vivo* into active metabolic intermediates. As these are unknown, it is too early to speculate over details on its exact metabolism, pharmacokinetics in animals and enrichment in specific tissues or degradation, although these issues are clearly important and will form part of our future studies. Ultimately, as the structure of these compounds provides considerable scope for modifications, and the synthesis of derivatives is now straight forward, this will become a promising starting point for future studies of structural variants.

2.3 | Molecular docking

Docking was performed to investigate the binding between the most active porphyrin derivatives (**2c**, **2d**, **2g**, and **2h**) and the two molecular targets: Bcl-2 and caspase-3. Since the experimental values presented in Figure 1 are for expression levels, they cannot be correlated to the binding affinities. Nevertheless, at least for caspase-3, porphyrins have been shown to have considerable binding using enzyme assays and molecular docking.[22] The predicted affinities for the most populated clusters per each docking calculation are shown in Table 4. Compounds **2d** and **2c** seem to have better affinities to both proteins than compounds **2g** and **2h**. As a representative for the two molecules with largest affinity, we further discuss the molecular interactions made by **2d** and the active site of each enzyme.

2.3.1 | Docking of 2d in caspase-3

It has been demonstrated that porphyrins fit well in the active site of caspase-3.[22] In accordance with the previous results, it seems that the porphyrin ring itself is not involved in strong interactions with the amino acids of the active site. Rather, it acts as a spacer to position H-bond donors and acceptors to interact with the side chains of arginine, serine, threonine and asparagine in the orthosteric active site of caspase-3. An illustration of the best pose of **2d** in the pocket of caspase-3 is given in Figure 2. A clearer 2D projection of the H-bonds network between **2d** and the surrounding amino acids is depicted in

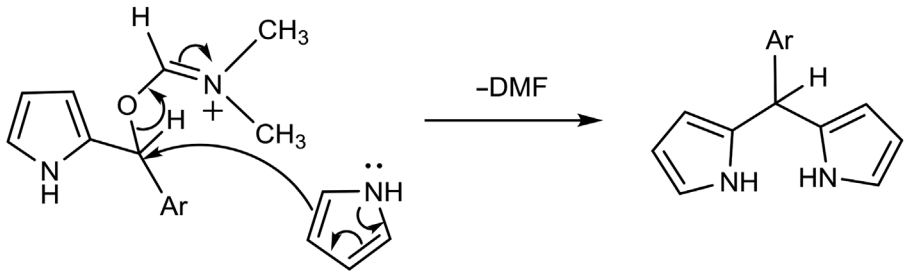

SCHEME 3 Proposed capping mechanism for the synthesis of porphyrin derivatives **2a–h** showing how DMF acts as a good leaving group as pyrrole is added

TABLE 1 The UV absorption bands of porphyrin derivatives **2a–h**

Compound	λ_{max} (nm)	log ε
2a	425	4.18
2b	427	4.30
2c	423	4.17
2d	426	4.23
2e	423	4.17
2f	425	4.22
2g	422	4.23
2h	427	4.30

Figure 3. The oxygen atoms in the sulfonamide groups act as H-bond acceptors, while the nitrogen atom acts as a H-bond donor. This rationalizes the low score obtained by compound **2g**, as it lacks any protruding H-bond donors or acceptors.

2.3.2 | Docking of 2d in Bcl-2

In contrast to caspase-3, porphyrins have not been reported to directly bind to the Bcl-2 protein. Rather, studies have been conducted on the interactions between porphyrins and the quadruplex DNA in the promoter region of *Bcl2*.[23] We herein, however, study the possibility of having interactions between the active site of Bcl-2 and porphyrin representatives. Similar to the docking in caspase-3, **2d** has the largest affinity to Bcl-2. The superposition of the best docking pose of **2d** and the co-crystallized ligand in the crystal structure demonstrates that the porphyrin fits properly in the active site of Bcl-2, see Figure 4. Nevertheless, the number of interactions made by **2d** and the amino acids in the active site are significantly less than those made by the native ligand. A 2D depiction of the interaction map is given in Figure 5. Similar to their role in the interaction with caspase-3, the sulfonamide groups of **2d** are involved in H-bonding with the neighboring amino acids while the porphyrin structure acts to position the H-bond donors and acceptors without being involved in major interactions (Figure 6).

TABLE 3 Cytotoxicity (IC_{50}) of tested compounds on different cancer cell lines

	IC_{50}[a] (μg/mL)			
Compound	HepG2	WI-38	Vero	MCF-7
2a	75	80	41	75
2b	26	51	44	35
2c	10	23	19	12
2d	9	21	17	9
2e	36	61	71	51
2f	31	61	69	54
2g	25	43	56	60
2h	12	24	12	18
5-Flu[b]	9	0	7	3

[a]IC_{50} (mg/mL): 1–10 (very strong), 11–25 (strong), 26–50 (moderate), 51–100 (weak), 100–200 (very weak), 200 (non-cytotoxicity).
[b]5-Flu = 5-fluorouracil.

3 | CONCLUSION

Although the eight porphyrin derivatives **2a–h** are new, they were synthesized via a new method, the capping mechanism, which led to high-yield porphyrins, and these derivatives were evaluated for antioxidant and antitumor activity in which compounds **2c**, **2d**, and **2h** showed strongest radical scavenging. On the other hand, compounds **2c**, **2d**, **2g**, and **2h** have very strong activity against HepG2 cell line with IC_{50} values from 9 to 25 μg/mL. Docking was performed to investigate the binding between the most active porphyrin derivatives (**2c**, **2d**, **2g**, and **2h**) and the two molecular targets: Bcl-2 and caspase-3.

TABLE 2 Antioxidant assay of the tested compounds relative to the standard commercial antioxidants BHA and BHT

Compound	DPPH (IC_{50}, mM/1 h)	HO (IC_{50}, mM)	LP (IC_{50}, mM)
2a	1.74	3.011	na[a]
2b	1.33	2.38	0.190
2c	0.061	0.230	0.030
2d	0.051	0.155	0.054
2e	2.60	1.520	na[a]
2f	1.320	1.930	0.190
2g	1.720	3.111	0.185
2h	0.098	0.210	0.053
BHA	0.012	2.130	0.048
BHT	0.040	1.940	0.210

BHA, 3-*tert*-butyl-4-hydroxyanisole; BHT, 3,5-di-*tert*-butyl-4-hydroxy-toluene; DPPH, 2,2-diphenyl-1-picrylhydrazyl; HO, hydroxyl; LP, lipid peroxidation.
[a]50% inhibition not achieved.

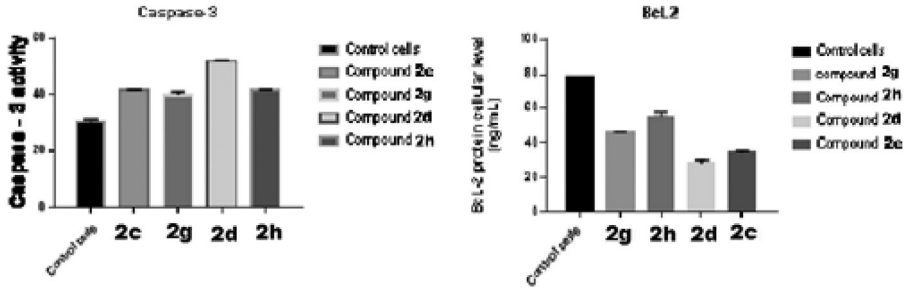

FIGURE 1 Expression levels of caspace-3 and Bcl-2 in HepG2 cells after 48 h incubation with **2c**, **2d**, **2g**, and **2h** at their respective IC_{50}s compared to unreacted cells

4 | EXPERIMENTAL

4.1 | Chemistry

4.1.1 | General

Gallenkamp electric melting point apparatus was used to determine melting points in degree centigrade, all melting points were uncorrected. Mattson 5000 FTIR spectrometer was used to record the IR spectra (KBr disk) at Mansoura University, Faculty of Science. Bruker WP 300, 200 MHz in DMSO as solvent was used to measure ^{1}H NMR spectra at Cairo University, Faculty of Science, Microanalytical Center. Unicam UV/Vis-spectrometer was used to record ultraviolet spectra at Mansoura University, Faculty of Science. Aldehydes: commercially available aldehydes were used as received. *m*-Aminobenzaldehyde was obtained from Aldlab Chemicals. 2,2,2-Trifluoro-*N*-(4-formylphenyl)acetamide was prepared according to the previously reported work (Richard P. Bonar-Law, *J. Org. Chem*., **1996**, *61*, 3623–3634).[30] *N*-(4-Formylphenyl)methanesulfonamide from Alfa Chemistry, *N*-(3-formylphenyl)methanesulfonamide from Sigma–Aldrich, *N*-formylpiperidine and *N*-formylmorpholine from Alfa Aesar. Julolidine-9-carbaldahyde was obtained from Tokyo Chemical Industry. *N*-Formylphenothiazine was prepared by traditional formylation method of Dűff ($POCl_3$/DMF at 100°C for 4 h).

The original spectra of the investigated compounds are provided as Supporting Information. The InChI codes of the compounds together with some biological activity data are also provided as Supporting Information.

TABLE 4 The docking scores of selected porphyrins in the active sites of caspase-3 and Bcl-2

Porphyrin	Docking scores for caspase-3 (kcal/mol)	Docking scores for Bcl-2 (kcal/mol)
2h	−7.6	−5.6
2d	−10.6	−10.7
2c	−10.1	−10.9
2g	−4.0	−9.8

4.1.2 | Synthesis of porphyrin derivatives 2a–h

Porphyrin derivatives **2a–h** were synthesized according to the previously reported work.[13]

5,10,15,20-Mesotetrakis(3-aminophenyl)-21*H*,23*H*-porphyrin (2a)

Yield 81%; m.p. 193°C; IR (KBr): v/cm^{-1} = 3350 (NH_2), 3250 (NH), 1661 (C═N), 1575 (C═C); ^{1}H NMR (DMSO-d_6) δ (ppm) = 5.22 (s, 8H, 4NH_2), 6.24 (d, 2H, pyrrolic CH), 6.38 (d, 2H, pyrrolic CH), 6.44 (d, 2H, pyrrolic CH), 6.78 (d, 1H, pyrrolic CH), 6.82 (d, 1H, pyrrolic CH), 6.62–7.82 (m, 12H, Ar-H), 8.89 (s, 1H, NH), 9.60 (s, 1H, NH); ^{13}C NMR: δ (ppm): 103.1, 118.3, 119.5, 120.98, 121.35, 123.1, 130.1, 131.1, 132.4, 136.5, 136.6, 140.9, 145.8, 153.7, 160.1; UV-vis. spectrum: (λ_{max}) 350, 425, 520, 550, 590, 650 nm. Anal. calcd. for $C_{44}H_{34}N_8$ (674.81): C, 78.32; H, 5.08; N, 16.61%. Found: C, 78.10; H, 4.99; N, 16.50%.

5,10,15,20-Mesotetrakis(4-trifluoro-acetamidophenyl)-21*H*,23*H*-porphyrin (2b)

Yield 76%; m.p. 171°C; IR (KBr): v/cm^{-1} = 3310 (NH), 1682 (CO), 1665 (C═N), 1580 (C═C); ^{1}H NMR (DMSO-d_6) δ (ppm) = 6.24 (d, 2H, pyrrolic CH), 6.26 (d, 2H, pyrrolic CH), 6.41 (d, 2H, pyrrolic CH), 6.52 (d, 2H, pyrrolic CH), 7.45–7.83 (m, 16H, Ar-H), 8.83 (s, 1H, NH), 9.62 (s, 1H, NH), 10.00 (s, 1H, NH-CO); ^{13}C NMR: δ (ppm): 103.1, 115.8, 119.5, 120.5, 122.0, 127.2, 129.8, 132.1, 136.7, 138.0, 141.1, 143.1, 155.0, 157.4, 161.1; UV-vis. spectrum: (λ_{max}) 360, 430, 520, 550, 595, 650 nm. Anal. calcd. for $C_{52}H_{30}N_8F_{12}O_4$ (1058.84): C, 58.99; H, 2.86; N, 10.58%. Found: C, 58.81; H, 2.77; N, 10.50%.

5,10,15,20-Mesotetrakis(4-methylsulfonamidophenyl)-21*H*,23*H*-porphyrin (2c)

Yield 71%; m.p. 210°C; IR (KBr): v/cm^{-1} = 3350 (NH), 1660 (CN), 1570 (CC), 1300 (SO_2); ^{1}H NMR (DMSO-d_6) δ (ppm) = 3.00 (s, 12H, 4CH_3), 6.22 (d, 2H, pyrrolic CH), 6.24 (d, 2H, pyrrolic CH), 6.40 (d, 2H, pyrrolic CH), 6.51 (d, 1H, pyrrolic CH), 6.91 (d, 1H, pyrrolic CH), 6.93–7.85 (m, 16H, Ar-H), 8.81 (s, 1H, NH), 9.63 (s, 1H, NH), 10.50 (s, 1H, $NHSO_2$); ^{13}C NMR: δ (ppm): 43,1, 103.1, 116.2, 119.7, 120.8, 128.1, 130.2, 132.3, 133.4, 136.0, 138.0, 141.1, 143.1, 155.7, 161.1; UV-vis. spectrum: (λ_{max}) 353, 425, 515, 550, 595, 650 nm. Anal. calcd. for

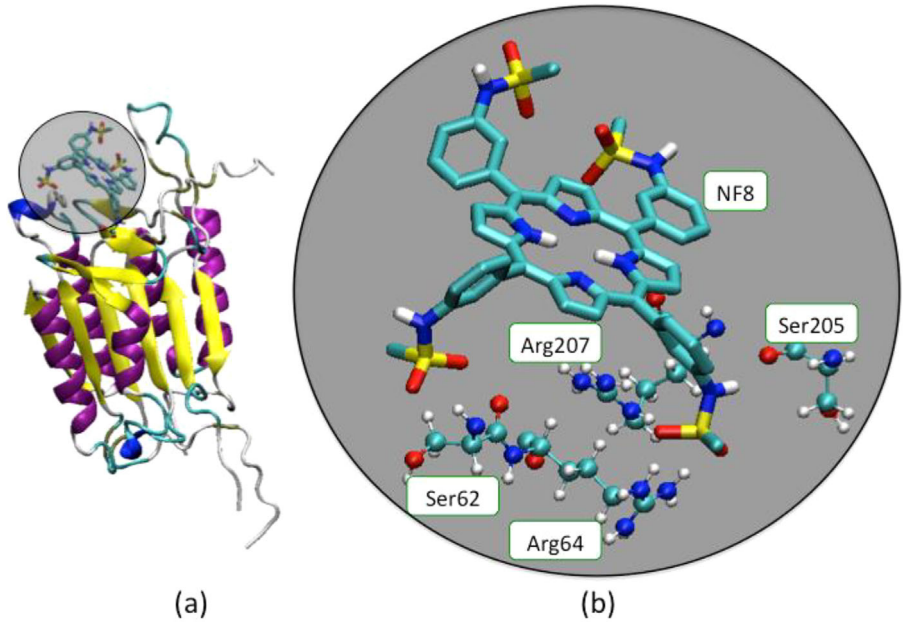

FIGURE 2 (a) The highest affinity docking pose of **2d** in the active site of caspase 3. (b) A zoom-in view showing the major amino acids interacting with **2d**

$C_{48}H_{42}N_8O_8S_4$ (987.15): C, 58.40; H, 4.29; N, 11.35%. Found: C, 58.33; H, 4.11; N, 11.21%.

5,10,15,20-Mesotetrakis(3-methylsulfonamidophenyl)-21*H*,23*H*-porphyrin (2d)

Yield 78%; m.p. 187°C; IR (KBr): ν/cm^{-1} = 3345 (NH), 1662 (C═N), 1571 (C═C), 1310 (SO_2); ^{1}H NMR (DMSO-d_6) δ (ppm) = 3.05 (s, 12H, $4CH_3$), 6.22 (d, 2H, pyrrolic CH), 6.24 (d, 2H, pyrrolic CH), 6.40 (d, 2H, pyrrolic CH), 6.49 (d, 1H, pyrrolic CH), 6.63 (d, 1H, pyrrolic CH), 6.65–7.82 (m, 16H, Ar-H), 8.89 (s, 1H, NH), 9.60 (s, 1H, NH), 10.54 (s, 1H, $NHSO_2$). UV-vis. spectrum: (λ_{max}) 360, 425, 515, 550, 595, 650 nm. Anal. calcd. for $C_{48}H_{42}N_8O_8S_4$ (987.15): C, 58.40; H, 4.29; N, 11.35%. Found: C, 58.32; H, 4.25; N, 11.31%.

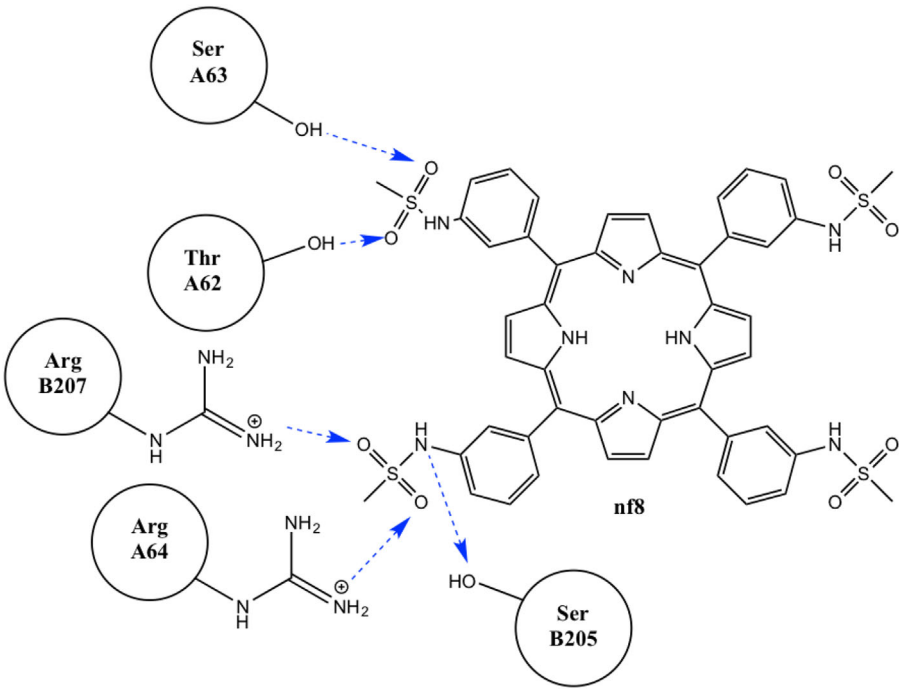

FIGURE 3 A 2D depiction of the interactions between **2d** and the active site of caspase, as illustrated in Figure 2

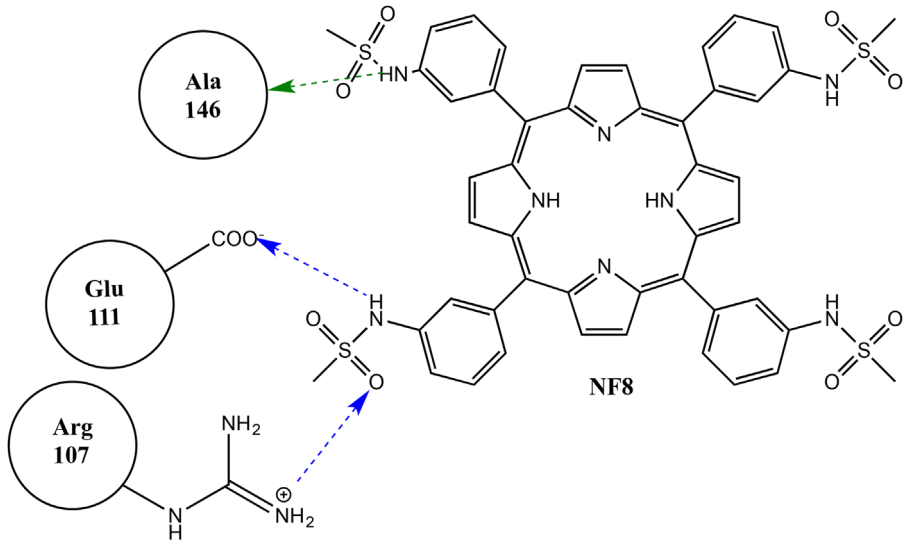

FIGURE 4 A 2D depiction of the interactions between **2d** and the active site of Bcl-2. The green arrow refers to an interaction with the backbone carbonyl of the alanine amino acid

5,10,15,20-Mesotetrakis(piperidin-1-yl)porphyrin (2e)

Yield 61%; m.p. 196°C; IR (KBr): ν/cm^{-1} = 3315 (NH), 1620 (C═N), 1580 (CC); ^{1}H NMR (DMSO-d_6) δ (ppm) = 1.12–1.41 (m, 24H, piperidine CH), 3.46 (t, 8H, piperidine CH), 3.65 (t, 8H, piperidine CH), 6.26 (d, 2H, pyrrolic CH), 6.40 (d, 2H, pyrrolic CH), 6.50 (d, 2H, pyrrolic CH), 7.80 (d, 2H, pyrrolic CH), 8.65 (s, 1H, NH), 9.60 (s, 1H, NH), 10.54 (s, 1H, $NHSO_2$); ^{13}C NMR: δ (ppm): 24.5, 26.1, 53.7, 58.5, 113.8, 114.7, 117.3, 119.9, 123.2, 125.1, 127.0, 139.9, 158.1. UV-vis. spectrum: (λ_{max}) 355, 450 nm. Anal. calcd. for $C_{40}H_{50}N_8$ (642.90): C, 74.73; H, 7.84; N, 17.43%. Found: C, 74.78; H, 7.73; N, 17.39%.

5,10,15,20-Mesotetrakis(morpholin-1-yl)porphyrin (2f)

Yield 70%; m.p. 221°C; IR (KBr): ν/cm^{-1} = 3310 (NH), 1625 (C═N), 1570 (C═C); ^{1}H NMR (DMSO-d_6) δ (ppm) = 3.55 (t, 16H, morpholinic CH), 3.85 (t, 16H, morpholinic CH), 6.24 (d, 2H, pyrrolic CH), 6.26 (d, 2H, pyrrolic CH), 6.40 (d, 2H, pyrrolic CH), 7.78 (d, 2H, pyrrolic CH), 8.84 (s, 1H, NH), 9.62 (s, 1H, NH); ^{13}C NMR: δ (ppm): 52.3, 53.3, 67.0, 113.8, 114.7, 117.3, 119.9, 123.2, 125.1, 127.0, 139.6, 158.1. UV-vis. spectrum: (λ_{max}) 355, 425 nm. Anal. calcd. for $C_{36}H_{42}N_8O_4$ (650.78): C, 66.44; H, 6.51; N, 17.22%. Found: C, 66.40; H, 6.47; N, 17.23%.

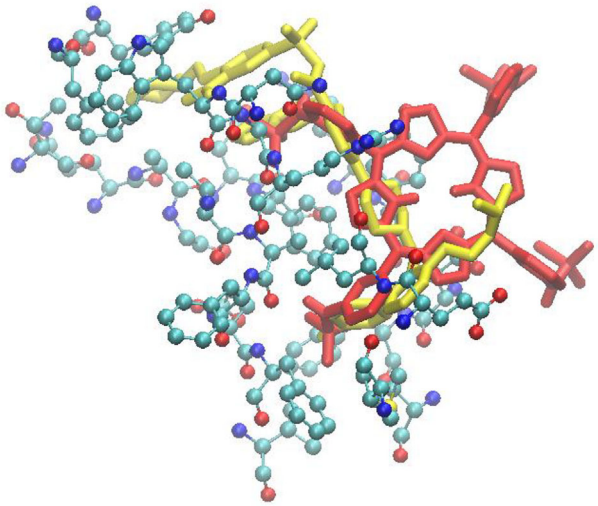

FIGURE 5 The superposition of the docked pose of **2d** (red) and the co-crystallized ligand (yellow) of the Bcl-2 crystal structure (PDB ID: 4MAN) with respect to the amino acids of the active site

5,10,15,20-Tetrakis(2,3,6,7-tetrahydro-1*H*,5*H*-pyrido[3,2,1-*ij*]quinolin-9-yl)porphyrin (2g)

Yield 65%; m.p. 263°C; IR (KBr): ν/cm^{-1} = 3333 (NH), 1621 (C═N), 1577 (C═C); ^{1}H NMR (DMSO-d_6) δ (ppm) = 1.96 (m, 16H, quinolinic CH), 2.79 (t, 16H, quinolinic CH), 3.37 (t, 16H, quinolinic CH), 6.24 (d, 2H, pyrrolic CH), 6.38 (d, 2H, pyrrolic CH), 6.44 (d, 2H, pyrrolic CH), 6.92 (s, 8H, Ar-H), 7.84 (d, 2H, pyrrolic CH), 8.87 (s, 1H, NH), 9.64 (s, 1H, NH). UV-vis. spectrum: (λ_{max}) 355, 427 nm. Anal. calcd. for $C_{68}H_{66}N_8$ (995.33): C, 82.06; H, 6.68; N, 11.26%. Found: C, 81.91; H, 6.58; N, 11.19%.

5,10,15,20-Tetra(10*H*-phenothiazin-10-yl)porphyrin (2h)

Yield 71%; m.p. 237°C; IR (KBr): ν/cm^{-1} = 3315 (NH), 1620 (C═N), 1585 (C═C); ^{13}C NMR: δ (ppm): 111.4, 114.8, 115.8, 118.3, 119.5, 120.5, 122.0, 123.2, 125.2, 127.2, 128.1, 132.2, 139.0, 140.6, 150.5. UV-vis. spectrum: (λ_{max}) 355, 427 nm. Anal. calcd. for $C_{68}H_{42}N_8S_4$ (1099.38): C, 74.29; H, 3.85; N, 10.19%. Found: C, 74.10; H, 3.78; N, 10.00%.

4.2 | Biochemical assays

4.2.1 | Antioxidant properties

The antioxidant properties were evaluated according to the reported method.[24]

4.2.2 | Cytotoxicity and antitumor assay

It was carried out according to the previously published work.[13]

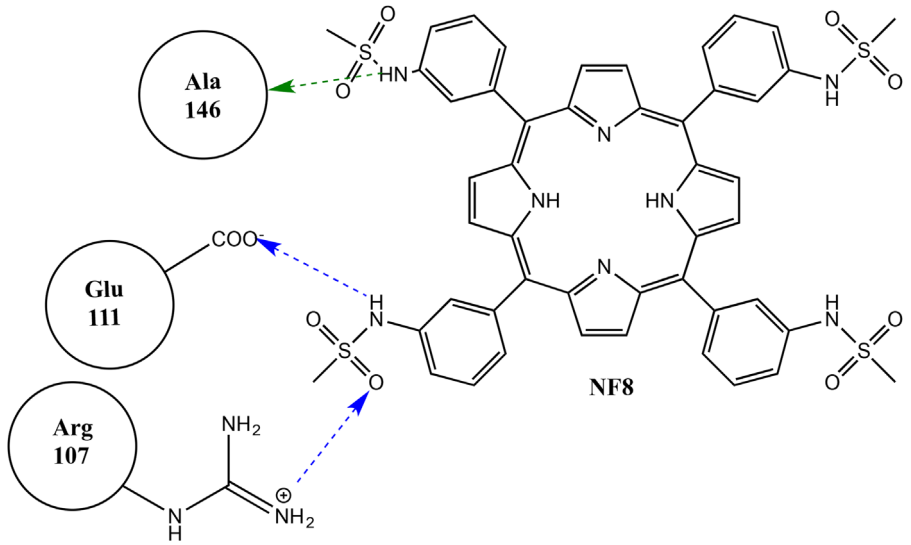

FIGURE 6 A 2D depiction of the interactions between **2d** and the active site of Bcl-2. The green arrow refers to an interaction with the backbone carbonyl of the alanine amino acid

4.2.3 | Detection of caspase-3 activity

Each IC_{50} of each compound was treated with HepG2 cells and incubated for 48 h. The cells were detached by trypsin and lysed by freezing at liquid nitrogen and then thawing with gentle mixing. Lysates cell was incubated with horseradish peroxidase (HRP) conjugated anti-CASP8 antibody for 30 min at 37°C. The end reaction product was recorded at 450 nm using enzyme-linked immunosorbent assay (Platinum ELISA; Biospes).

4.2.4 | Detection of Bcl-2 protein levels

Bcl-2 levels were evaluated in HepG2 cells treated with the corresponding IC_{50} of each compound and incubated for 48 h and compared with their levels in control untreated HepG2 cell line. The cells were harvested by applying trypsin and lysed by freezing with liquid nitrogen and then thawing with gentle mixing. According to the instructions of the manufacturer of (Platinum ELISA; eBioscience©), cell lysates were incubated with biotin-conjugate for 2 h at 25°C and then with streptavidin-HRP for 1 h at 25°C. The reaction product was detected at 450 nm.

4.3 | Molecular docking

The porphyrin structures were optimized using GAMESS software[25] at the HF/6-31 level. The optimized structures were used in various dockings. All dockings were done using AutoDock4[26] keeping side chains at the active site rigid. The bonds in the porphyrin ring were also rendered rigid during docking. We used the crystal structure 4MAN[27] and 6BFJ[28] for Bcl-2 and caspase-3, respectively. Docking was performed using 100 steps of genetic algorithm while keeping all the default settings provided by AutoDock Tools. Visualization was done using VMD.[29]

CONFLICT OF INTEREST

The author declares that there is no conflict of interest.

ORCID

Sraa Abu-Melha http://orcid.org/0000-0001-5539-0163

REFERENCES

[1] *Porphyrins and Metalloporphyrins* (Ed: K. M. Smith), Elsevier, The Netherlands **1976**, pp. 29–58.
[2] K. M. Kanish, K. M. Smith, R. Guilard, *The Porphyrin Handbook*, Vol. 6, Academic Press, San Diego **2000**, pp. 45–118.
[3] R. F. Barth, A. H. Soloway, J. H. Goodman, R. A. Gahbauer, *Neurosurgery* **1999**, *44*, 433.
[4] K. J. Barnham, C. I. Masters, A. I. Bush, *Nat. Rev. Drug Discov.* **2004**, *3*, 205.
[5] a) M. S. Cooke, M. D. Evans, M. Dizdaroglu, J. Lunez, *FASEB J.* **2003**, *17*, 1195; b) T. Finkel, N. G. Holbrook, *Nature* **2000**, *408*, 239; c) S. P. Hussain, L. J. Hofseth, C. C. Harris, *Nat. Rev. Cancer* **2003**, *3*, 276.
[6] a) Y.-J. Cai, L. P. Ma, L. F. Hou, B. Zhou, L. Yang, Z.-L. Liu, *Chem. Phys. Lipids* **2002**, *120*, 109; b) B. Zhou, Q. Miao, L. Yang, Z.-L. Liu, *Chem. Eur. J.* **2005**, *11*, 680; c) B. Zhou, L.-M. Wu, L. Yang, Z.-L. Liu, *Free Radical Biol. Med.* **2005**, *38*, 78.
[7] Y. J. Cai, J. G. Fang, L. P. Ma, L. Yang, Z.-L. Liu, *Biochim. Biophys. Acta* **2003**, *1637*, 31.
[8] D. Holten, D. F. Bocian, J. S. Lindsey, *Acc. Chem. Res.* **2002**, *35*(1), 57.
[9] O. Mongin, A. Schuwey, M. A. Vallot, A. Gossauer, *Tetrahedron Lett.* **1999**, *40*, 8347.
[10] A. Dudkowiak, E. Teslak, J. Habdas, *J. Mol. Struct.* **2006**, *792–793*, 93.
[11] G. Mele, R. Del Sole, G. Vasapollo, E. Garcia-Lopez, *J. Catal.* **2003**, *217*(2), 334.
[12] C. S. Chan, K. S. Chan, *J. Org. Chem.* **1994**, *59*, 6084.
[13] A. A. Fadda, R. E. El-Mekawy, A. I. El-Shafei, H. Freeman, *Arch. Pharm. Chem Life Sci.* **2013**, *346*, 53.

[14] S. Shaaban, A. Negm, M. A. Sobh, L. A. Wessjohann, *Anti-Cancer Agents Med. Chem*. **2016**, *16*, 621.
[15] N. Mimica-Dukin, B. Bozin, M. Sokolovic, N. Simin, *J. Agric. Food Chem*. **2004**, *52*, 2485.
[16] N. A. Abbas, S. Shaaban, H. E. Gaffer, E. Abdel-Latif, *Res. J. Pharm. Biol. Chem. Sci*. **2015**, *6*, 1655.
[17] S. Shaaban, F. Sasse, T. Burkholz, C. Jacob, *Bioorg. Med. Chem*. **2014**, *22*, 3610.
[18] B. F. Abdel-Wahab, S. Shabaan, *Synthesis* **2014**, *46*, 1709.
[19] S. Shaaban, R. Diestel, B. Hinkelmann, Y. Muthukumar, R. P. Verma, F. Sasse, C. Jacob, *Eur. J. Med. Chem*. **2013**, *58*, 192.
[20] A. A. Fadda, R. E. El-Mekawy, A. I. El-Shafei, *J. Porphyr. Phthalocyanines* **2015**, *19*, 735.
[21] A. A. Fadda, R. E. El-Mekawy, A. I. El-Shafei, *J. Chem*. **2013**, *2013*, 1.
[22] S. B. Blumenthal, A. K. Kiemer, G. Tiegs, S. Seyfried, M. Holtje, B. Brandt, H.-D. Holtje, S. Zahler, A. M. Vollmar, *FASEB J*. **2005**, *19*, 1272.
[23] M. del Toro, P. Bucek, A. Aviñó, J. Jaumot, C. González, R. Eritja, R. Gargallo, *Biochimie* **2009**, *91*, 894.
[24] A. A. Fadda, R. E. El-Mekawy, N. N. Soliman, A. M. Allam, M. T. Abdelaal, *Dyes Pigments* **2018**, *155*, 300.
[25] M. W. Schmidt, K. K. Baldridge, J. A. Boatz, S. T. Elbert, M. S. Gordon, J. J. Jensen, S. Koseki, N. Matsunaga, K. A. Nguyen, S. Su, T. L. Windus, M. Dupuis, J. A. Montgomery, *J. Comput. Chem*. **1993**, *14*, 1347.
[26] G. M. Morris, R. Huey, W. Lindstrom, M. F. Sanner, R. k. Belew, D. S. Goodsell, A. J. Olson, *J. Comput. Chem*. **2009**, *30*, 2785.
[27] A. J. Souers, J. D. Leverson, S. W. Elmore, *Nat. Med*. **2013**, *19*, 202.
[28] M. E. Thomas, R. Grinshpon, P. Swartz, A. C. Clark, *J. Biol. Chem*. **2018**, *293*, 5447.
[29] W. Humphrey, A. Dalke, K. Schulten, *J. Mol. Graph* **1996**, *14*, 33.
[30] R. P. Bonar-Law, *J. Org. Chem*. **1996**, *61*, 3623.

SUPPORTING INFORMATION

Additional supporting information may be found online in the Supporting Information section at the end of the article.

How to cite this article: Abu-Melha S. Efficient synthesis of *meso*-substituted porphyrins and molecular docking as potential new antioxidant and cytotoxicity agents. *Arch Pharm Chem Life Sci*. 2018;1–10.
https://doi.org/10.1002/ardp.201800221